



Cell-binding IgM in CSF is distinctive of multiple sclerosis and targets the iron transporter SCARA5

Ilaria Callegari,^{1,2} Johanna Oechtering,² Mika Schneider,¹ Sylvain Perriot,³ Amandine Mathias,³ Margarete M. Voortman,⁴ Alessandro Cagol,^{2,5} Ulrike Lanner,⁶ Martin Diebold,^{2,7} Sebastian Holdermann,¹ Victor Kreiner,⁸ Burkhard Becher,⁸ Cristina Granziera,^{2,5} Andreas Junker,⁹ Renaud Du Pasquier,^{3,10} Michael Khalil,⁴ Jens Kuhle,² Ludwig Kappos,² Nicholas S. R. Sanderson^{1,2,†} and Tobias Derfuss^{1,2,†}

†These authors contributed equally to this work.

Intrathecal IgM production in multiple sclerosis is associated with a worse disease course. To investigate pathogenic relevance of autoreactive IgM in multiple sclerosis, CSF from two independent cohorts, including multiple sclerosis patients and controls, were screened for antibody binding to induced pluripotent stem cell-derived neurons and astrocytes, and a panel of CNS-related cell lines. IgM binding to a primitive neuro-ectodermal tumour cell line discriminated 10% of multiple sclerosis donors from controls. Transcriptomes of single IgM producing CSF B cells from patients with cell-binding IgM were sequenced and used to produce recombinant monoclonal antibodies for characterization and antigen identification. We produced five cell-binding recombinant IgM antibodies, of which one, cloned from an HLA-DR+ plasma-like B cell, mediated antigen-dependent complement activation. Immunoprecipitation and mass spectrometry, and biochemical and transcriptome analysis of the target cells identified the iron transport scavenger protein SCARA5 as the antigen target of this antibody. Intrathecal injection of a SCARA5 antibody led to an increased T cell infiltration in an experimental autoimmune encephalomyelitis (EAE) model. CSF IgM might contribute to CNS inflammation in multiple sclerosis by binding to cell surface antigens like SCARA5 and activating complement, or by facilitating immune cell migration into the brain.

1 Department of Biomedicine, University of Basel and University Hospital Basel, Basel 4031, Switzerland

2 Neurologic Clinic and Policlinic, MS Center and Research Center for Clinical Neuroimmunology and Neuroscience Basel (RC2NB), University Hospital Basel and University of Basel, Basel 4056, Switzerland

3 Department of Clinical Neurosciences, Laboratory of Neuroimmunology, Center of Research in Neurosciences, Lausanne 1011, Switzerland

4 Department of Neurology, Medical University of Graz, Graz 8010, Austria

5 Translational Imaging in Neurology (ThINK) Basel, Department of Biomedical Engineering, Faculty of Medicine, University Hospital Basel, University of Basel, Basel 4123, Switzerland

6 Proteomics Core Facility, Biozentrum, University of Basel, Basel 4056, Switzerland

7 Institute of Neuropathology, Faculty of Medicine, University of Freiburg, Freiburg 79085, Germany

8 Institute of Experimental Immunology, University of Zurich, Zurich 8057, Switzerland

9 Department of Neuropathology, University Hospital Essen, Essen 45147, Germany

10 Department of Clinical Neurosciences, Service of Neurology, Lausanne 1011, Switzerland

Received April 05, 2023. Revised October 27, 2023. Accepted November 05, 2023. Advance access publication December 20, 2023

© The Author(s) 2023. Published by Oxford University Press on behalf of the Guarantors of Brain.

This is an Open Access article distributed under the terms of the Creative Commons Attribution-NonCommercial License (<https://creativecommons.org/licenses/by-nc/4.0/>), which permits non-commercial re-use, distribution, and reproduction in any medium, provided the original work is properly cited. For commercial re-use, please contact journals.permissions@oup.com

Correspondence to: Nicholas S. R. Sanderson
 Department of Biomedicine, Hebelstrasse 20, 4031 Basel, Switzerland
 E-mail: nicholas.sanderson@unibas.ch

Keywords: complement; immunoprecipitation; plasma cells; iron metabolism

Introduction

One of the diagnostic hallmarks of multiple sclerosis (MS) is intrathecal immunoglobulin production, identifiable at CSF examination as oligoclonal IgG bands (OCB). Other than in MS, OCB are found in CNS inflammatory conditions and when the cause is infectious, antibodies that are specific for the causal pathogen can be identified amongst those constituting the OCB.^{1,2}

The prevalent class of intrathecally produced antibodies is IgG,³ but intrathecally produced IgM is also present in 20–25% of patients,⁴ and their presence has been associated with more active and severe disease^{4–8}. IgM sequences from the CSF of patients with MS or neuroborreliosis show a high degree of somatic hypermutation, suggesting an antigen-driven IgM response,⁹ rather than a bystander response. In MS, comparison of the immunoglobulin transcriptomes of B cells in CSF and in lesions with peptide sequences of soluble CSF antibodies suggests that all three are clonally related.^{10,11} Known mechanisms by which IgM might damage brain tissue are dependent on antigen recognition and binding, implying that if IgM is causally involved in pathogenesis, it must bind antigens in the CNS. By analogy with established pathogenic auto-antibodies, we expect such antibodies to bind conformational epitopes on the surface of live cells.¹² A result consistent with this prediction was indeed observed by Lily *et al.*,¹³ who saw that antibodies from serum or CSF from patients with MS had a stronger propensity to bind to human oligodendrocyte and neuronal cell types than samples from healthy patients.

We therefore screened CSF from patients with MS and controls for antibodies of different classes that bind to live, CNS-related cell types. Having discovered an MS-restricted IgM binding pattern, we then set about identifying the target and characterizing the pathogenic B cell phenotype.

Materials and methods

Methods

Methods are described in detail in the [Supplementary material](#).

Patient samples

CSF samples from patients undergoing diagnostic lumbar puncture at the University Hospital Basel and from University Hospital of Graz were collected and immediately processed. All procedures were approved by the Ethical Committee of Northwest Switzerland (study protocol 2021-00908) and by the Ethical Committee of the Medical University of Graz, Austria (study protocol 17-046 ex 05/06 and 31-432 ex 18/19). Each sample was collected using a 15 ml falcon tube, centrifuged at 400g at room temperature for 10 min; the CSF supernatant was then aliquoted and frozen at –80°C. For the prospective part of the study, the CSF samples were analysed for cell line-binding IgM by flow cytometry, immediately after collection, and the CSF cell pellet was resuspended in RPMI supplemented with 40% fetal calf serum (FCS) (R40) and kept on ice for further processing or stored within 2 h in liquid nitrogen.

Cell lines

Cell lines used are described in [Supplementary Table 1](#).

Statistics

Differences between conditions were tested for deviation from normality, when normal were subjected to analysis of variance, and when significantly deviated from normal to appropriate non-parametric tests, as specified in the figure legends.

Results

IgM but not IgG binding to PNET cells discriminates multiple sclerosis patients from controls

First we screened CSF samples from 128 patients with MS and 142 controls for IgM binding to neurons and astrocytes derived from human induced pluripotent stem cells (iPSCs) by flow cytometry, blinded to the diagnosis. Overall IgM binding was not obviously different between patients and controls ([Fig. 1A](#)), but some samples showed an MS-specific pattern of antibody binding to a subset of cells ([Supplementary Fig. 1A and B](#)). This subset was too small to be easily used for downstream studies and we therefore screened the same cohort of CSF, plus an additional 44 MS samples and 50 control samples ([Supplementary Table 2](#)) against a panel of CNS-related tumour cell lines ([Supplementary Table 1](#)).

IgM binding varied both by disease status and by cell line ([Fig. 1B–D](#)). In particular, cells from the PNET and STTG1 lines were bound by IgM from CSF of patients with either clinically isolated syndrome (CIS) or MS, but not by IgM from control CSF ([Fig. 1B–D](#)). The PNET cell line was recognized by IgM from CSF from ~10% of MS patients and <1% of control samples, and this signal was not correlated with intrathecal IgM concentration—even among controls with relatively high levels of intrathecal IgM production, with one exception, no PNET-binding IgM was detected ([Fig. 1C](#)). CSF from six donors with MS contained cell-binding IgG, but this was discovered to result from therapeutically administered natalizumab, as recently described,¹⁴ and these samples were therefore excluded from further analysis. Otherwise, CSF IgG was not different between patients with MS and controls ([Fig. 1D](#)).

For a subset of cell lines, including PNET, we examined binding of IgM and IgG from sera from the same donors. Both were similar across cell lines and between patients with MS and controls ([Supplementary Fig. 1C](#)).

To confirm the MS-specific IgM binding pattern observed in CSF from the Basel cohort, we repeated the study using CSF samples from a cohort from an independent centre (University Hospital of Graz, Austria). Samples (MS/CIS = 100, control = 100) were shipped coded and analysed by investigators unaware of diagnoses. Results replicated those from the Basel cohort ([Supplementary Fig. 1D and E](#)). IgM binding to the PNET cell line was more commonly observed in patients with MS/CIS diagnosis, (CIS > control, $P < 0.0001$, one-way, ANOVA) and after exclusion of two donors with therapeutic natalizumab detected, no disease-specific pattern was seen for IgG.

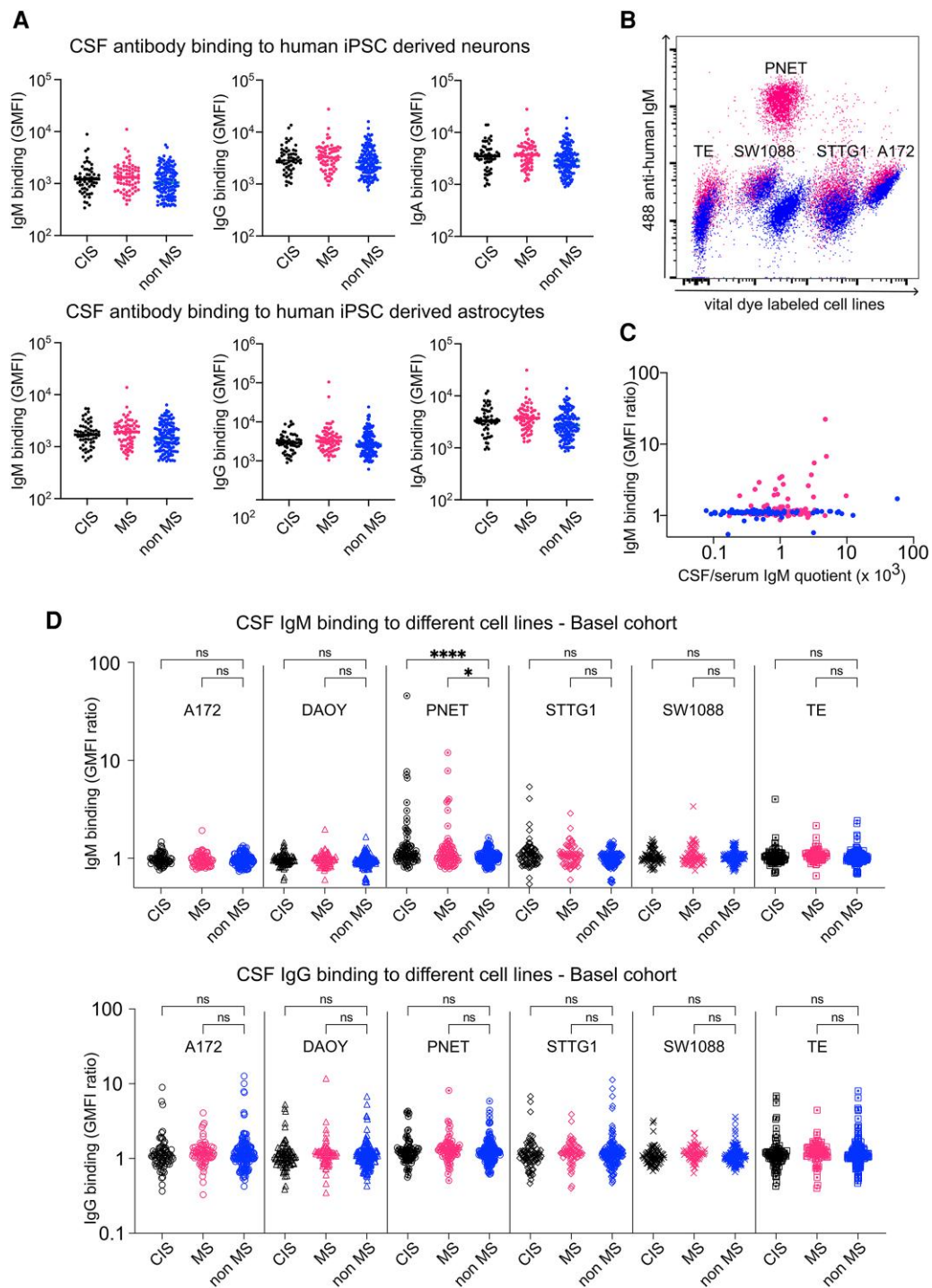


Figure 1 Binding of antibodies from CSF to live cells. (A) Binding of antibodies from CSF to astrocytes or neurons derived from human induced pluripotent stem cells (iPSCs). Each column scatter plot shows results for CSF samples from donors with a diagnosis of clinically isolated syndrome (CIS), clinically definite multiple sclerosis (MS), or controls. Upper row of plots shows binding to neurons and lower plots binding to astrocytes. Plots on left show IgM, plots in middle show IgG and plots on right show IgA. Each dot represents one sample. Vertical axis shows geometric mean fluorescence intensity. Results from CSF samples from donors with CIS are shown in black, MS in red, and controls in blue. (B) Exemplary flow cytometry dot plot comparing IgM binding from CSF against the indicated cell lines. The vertical axis shows the fluorescence intensity of the secondary antibody used to detect the bound antibody, and the horizontal axis shows the intensity of the fluorescent vital dye Cell Trace Violet used to label the various cell lines before mixing, to enable their subsequent separation. Red dot plot shows IgM binding from CSF donated by a patient with CIS. Blue dot plot shows results with secondary antibody only. (C) Relationship between PNET-binding IgM signal (vertical axis, GMFI ratio) and CSF/serum IgM quotient (horizontal axis) (Pearson $r = 0.096$, $P = 0.176$). (D) Binding of antibodies from CSF to various cell lines. Vertical axis shows GMFI ratio (antibody + secondary-labelled cells divided by cells labelled with secondary antibody only). The 18 columns represent binding of IgM (upper row) or IgG (lower row) from CSF samples from donors in Basel with CIS (black), MS (red) and controls (blue) to each of six cell lines whose names are shown inside each plot. One-way ANOVA * $P = 0.049$, **** $P < 0.0001$. ns = not significant.

Looking at clinical characteristics, those donors with anti-PNET IgM in their CSF were—on average—younger than negative donors, had more cells in CSF, and were more likely to have oligoclonal bands (Supplementary Table 3).

Cloning and characterization of PNET-specific CSF IgM antibodies

We prospectively screened CSF from a total of 212 patients for PNET binding. From one donor whose CSF contained PNET-binding IgM (Supplementary Fig. 2A), 1678 CD19+ B cells were sorted and cultured (Supplementary Fig. 2B). Five single B cell supernatants contained PNET-binding IgM (Fig. 2A and Supplementary Fig. 2C). Transcriptomes of these B cells were surveyed by RNA sequencing and immunoglobulin gene sequences were cloned (Supplementary Table 4). One antibody (B3) showed the PNET-specific binding pattern of the original CSF (Fig. 2B and C).

The five antibodies had various levels of somatic hypermutation (Supplementary Table 4). Following Beltran *et al.*,⁹ we examined the ratio of silent to replacement mutations of the immunoglobulin gene. We found an increased rate of replacement mutations in the complementarity-determining region (CDR) of B3 (6.5) compared to the FR (1.4) indicating an antigen-driven mutation of this B cell clone.

To further examine this inference, we tested the binding of a de-mutated version of the antibody, in which one or both of the chains were generated in their inferred germline sequences. Reversion of only the light chain partially reduced PNET binding, while reversion of the heavy chain completely eliminated it (Fig. 2D).

To gain some insight into the phenotype of the B cell that produced the B3 antibody, we compared its transcriptome with that of the other B cells that had undergone the same single cell transcriptomics protocol. B3 is characterized by an unusual combination of plasma cell markers such as PRMD1, IRF4, MZB1, GPR183 and JCHAIN, with genes related to antigen presentation, such as HLA molecules, CD74 and CD53 (Fig. 2E and Supplementary Table 5).

We also exploited complement activation as a measure of antigen-specificity. We observed that B3 was able to induce C3b deposition on the PNET cell surface (Fig. 2F) but the PNET-non-specific and less mutated M16, was not.

The molecular target of B3

B3 binding geometric mean fluorescence index (GMFI) was reduced by roughly 10-fold following protease treatment (Fig. 3A), suggesting specific recognition of a cell surface protein. On the other hand, deglycosylation with various endoglycosylases did not affect the binding (Fig. 3A and Supplementary Fig. 3). To directly investigate the antigenic target of B3, we used immunoprecipitation followed by mass spectrometry. This method has mostly been used with IgG, but artificially class-switching B3 to IgG compromised binding to PNET cells (Supplementary Fig. 4A). We therefore adapted the technique for

IgM using magnetic beads coated with anti-human IgM. We confirmed immunoprecipitation of haemagglutinin from transfected cells using a monoclonal anti-HA IgM (Supplementary Fig. 4B) and then applied the method to immunoprecipitate the target of B3 from PNET cells. Three independent experiments, with a total of seven replicates, identified several differentially retrieved proteins, and when these results were restricted to only those with the gene ontology (GO) term 'plasma membrane', the most obvious candidate was SCARA5 (Fig. 3B and Supplementary Fig. 4C). In addition to the immunoprecipitation approach, we also reasoned that the specificity of the B3 antibody for the PNET cell line ought to be reflected in PNET-specific expression of the antigen, and we accordingly examined the whole transcriptome of each of the 13 cell lines, including PNET cell and the 12 non-bound cell lines (Fig. 3C). Several dozen genes were almost exclusively expressed in PNET cells and narrowing the search to plasma membrane proteins significantly more highly expressed in PNET than other cell lines yielded 30 candidates, including SCARA5 (Fig. 3C).

From these results, two genes appeared as plausible candidates, the iron transport scavenger protein SCARA5 and the protocadherin PCDH18. Flow cytometry with transiently transfected cells showed no specific binding of B3 to PCDH18-transfected cells, but clear binding to the SCARA5 transfected cells (Fig. 3D). PNET cells express three isoforms of SCARA5, with 495, 400 and 176 amino acids, and we repeated the flow cytometry screen with each. The two longer isoforms were clearly bound, while isoform 176 had binding no higher than untransfected cells (Fig. 3E). We confirmed the antigenicity of the transfected SCARA5 with commercially available antibodies and tested whether the epitope bound by B3 overlapped with these antibodies (Supplementary Table 6). The commercial monoclonal and polyclonal antibodies, and B3, all had individual, non-overlapping epitopes.

Antigen validation and cohort screening

To test whether the newly identified antigen explains the PNET IgM reactivity we observed in the CSF of MS patients, we screened a cohort of 307 CSF samples [87 with relapsing remitting MS (RRMS), 116 with CIS, 23 with secondary progressive MS (SPMS), 14 with primary progressive MS (PPMS), 27 from inflammatory controls and 40 from non-inflammatory controls] for the presence of antibodies binding to PNET cells, or to HEK cells transfected with 495 or 176 amino acid isoforms of SCARA5. We confirmed the binding of CSF IgM to PNET cells in 11% of CIS patients, 10% of RRMS patients and 3% of control subjects. In one RRMS case, IgM binding to PNET cells also bound to SCARA5 isoform 495. None of the PPMS, SPMS or non-inflammatory controls showed reactivity against PNET cells or cells expressing SCARA5 isoform 495 (Fig. 3F). We also tested the serum reactivity against SCARA5-transfected HEK cells for a subset of donors and found only one donor (distinct from the donor with anti-SCARA5 IgM in CSF) with detectable anti-SCARA5 IgM in serum (Fig. 3G).

Figure 2 Continued

fully germline reverted version. (E) Transcriptional characteristics of B cell B3. cDNA from each of five singly cultured B cells was subjected to Illumina sequencing and for each gene observed, the log₁₀ number of reads found in B3 was plotted against the log₁₀ mean number of reads found in the other B cells (blue dots). Genes whose expression is >5-fold higher in B3 are marked with red circles and for a subset, their gene symbols printed beside the plotted dots. This information for all the B3 overabundant genes is collated in Supplementary Table 5. Genes regarded as plasma cell markers have their symbols in black, genes associated with antigen presentation in dark blue. (F) Antibody-dependent complement activation mediated by B3. PNET cells were incubated with monoclonal IgM B3, or with M16, in the presence of human serum from a healthy donor as a source of complement. Serum only without additional antibody was used as a control. Antibody-dependent complement activation was detected by bound C3 immunolabeling flow cytometry. Vertical axis shows GMFI ratio. *P = 0.0385, one-way ANOVA. ns = not significant.

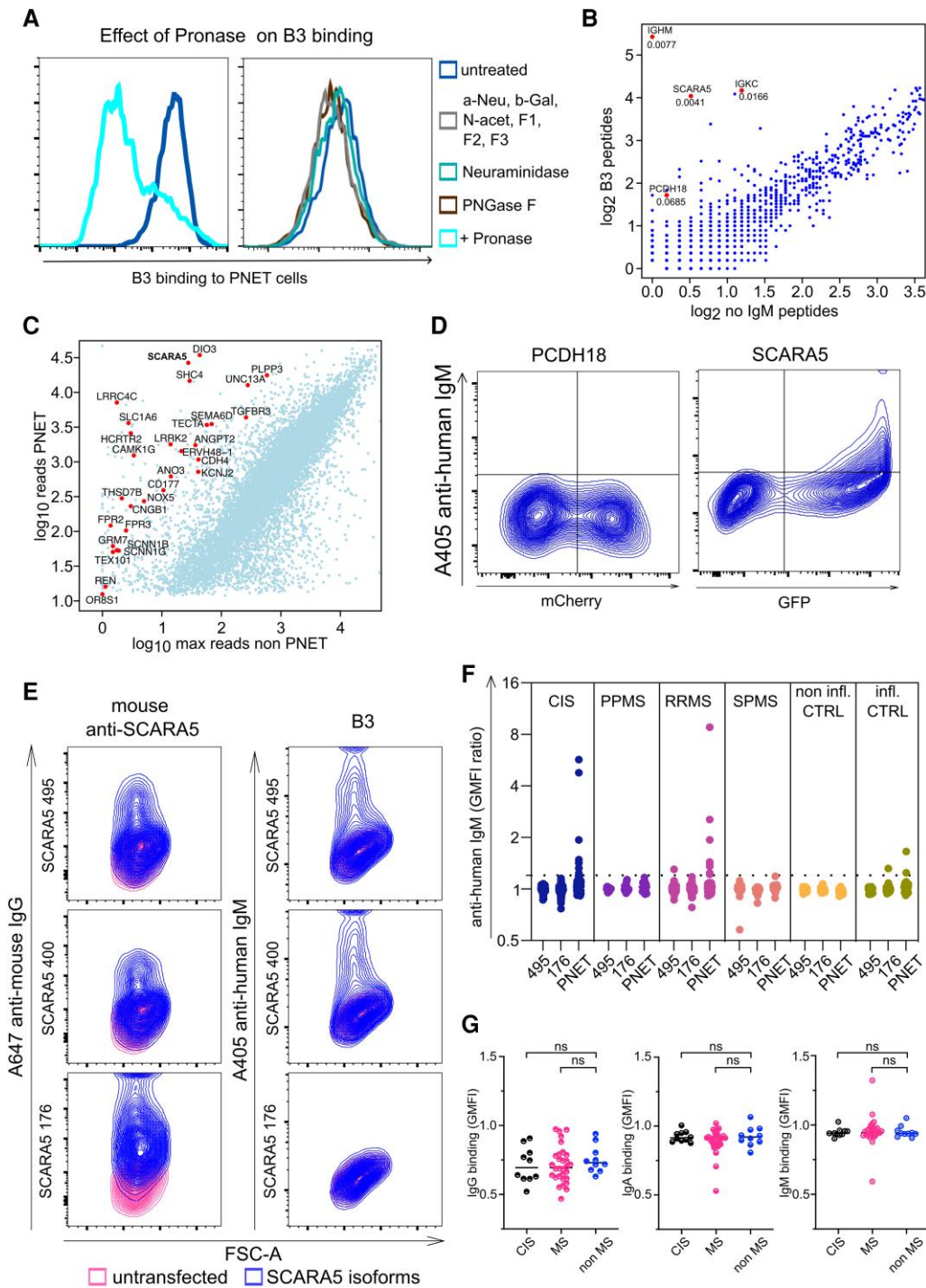


Figure 3 Target antigen of IgM B3. (A) Effects of protease treatment or deglycosylation on B3 binding. Histogram on left shows binding to untreated PNET cells in dark blue and binding to cells treated with the non-specific protease mixture Pronase to cleave exposed cell surface proteins in light blue. Histogram on right shows the effect of deglycosylation treatment on B3 binding. Binding to untreated PNET cells is shown in dark blue, binding to cells treated with various deglycosylating enzymes to specifically cleave terminal sugar moieties from cell surface carbohydrates is shown with other coloured histograms, as specified on right of plot. Specificity controls for deglycosylation treatments are shown in [Supplementary Fig. 3](#). (B) Immunoprecipitation and mass spectrometry to identify the unknown protein target of the PNET-binding IgM B3. Live PNET cells were first incubated with B3, then washed and lysed; the lysate was next incubated with anti-IgM coated Dynabeads, washed and magnetically retrieved. Proteins were eluted from the beads, digested with trypsin, and peptides detected by mass spectrometry. Data are pooled from three independent experiments. Vertical axis shows log₂ number of peptides precipitated by B3. Horizontal axis shows same parameter from control preparation in which the B3 was omitted. Each dot is one protein. Red dots are proteins whose retrieval was significantly more likely in the B3 samples (two-tailed unpaired t-test, $P < 0.1$), filtered for only those genes whose gene ontology (GO) terms include ‘plasma membrane’. These proteins are labelled with their gene symbol and the P -value is shown below each symbol. (C) Transcriptional characteristics of the PNET cell line bound by B3. cDNA from each of 13 cell lines was subjected to illumina sequencing and for each gene observed, the log₁₀ number of reads found in the PNET cell lines was plotted against

(Continued)

For a subset of donors, we compared the anti-PNET IgM signal with the abundance of paramagnetic rim lesions, as assessed by MRI, but there was no significant difference in this parameter between positive and negative donors (Supplementary Table 3).

Anti-SCARA5 antibodies influence leucocyte trafficking into the CNS

To investigate possible mechanisms by which antibodies against SCARA5 might influence the autoreactive immune response, we examined the expression of SCARA5 in autoptic brain lesions from MS donors by immunolabelling with a rabbit polyclonal anti-SCARA5 antibody. Most intense labelling was observed on foamy macrophages adjacent to active lesions, but weaker labelling was also found associated with neurons and astrocytes around chronic MS lesions (Supplementary Figs 5 and 6A). Occasionally, SCARA5 labelling overlapped with IgM deposition in MS lesions (Supplementary Fig. 6B). To corroborate these results, we interrogated publicly available databases of single cell RNA expression data bioinformatically. This approach showed expression of SCARA5 RNA in GABAergic interneurons, mesenchymal cells of the choroid plexus, and endothelial cells (Supplementary Fig. 6C). Immunolabelling of mouse brains showed strongest expression in the periventricular and subdural blood vessels, and in the choroid plexus (Fig. 4A). In view of the importance of blood vessels and the choroid plexus in immune cell trafficking into the CNS,¹⁴ we hypothesized that anti-SCARA5 antibodies might exert their pathogenic effect by perturbing immune cell migration. We confirmed that anti-SCARA5 antibodies injected directly into the lateral ventricle bind to periventricular blood vessels *in vivo* (Fig. 4B) and then examined the effect of this manipulation on immune cell trafficking (Fig. 4C). We transferred activated 2D2 T cells, specific for the myelin protein myelin oligodendrocyte glycoprotein (MOG) into mice, and as the first animal manifested motor signs, we injected half of the animals with polyclonal sheep anti-SCARA5 IgG (the patient-derived antibody B3 is human-specific), or control antibody (polyclonal sheep anti-influenza neuraminidase IgG) into the lateral ventricle. We tracked the motor behaviour and weights of the animals (Fig. 4D and E), and 1 week later we sacrificed the animals and quantified T cells in the brain by immunofluorescence microscopy. T cell infiltration in the perivascular areas adjacent to the injection site was significantly augmented by anti-SCARA5 antibodies (Fig. 4F and G).

Discussion

Antibodies are produced intrathecally in several CNS disorders and OCB are found in the CSF of more than 90% of patients with MS.^{3,8} The most obvious outstanding question about CSF antibodies in MS concerns their target antigen(s).

In this study, we aimed to identify the target of intrathecally produced immunoglobulins by screening them against multiple neuronal cell lines and human iPSC-derived neurons and astrocytes. At the population level, we identified an IgM signal in CSF that discriminated MS patients from controls. From a single B cell of a patient whose CSF showed this signal, we isolated a monoclonal antibody and identified its molecular target as the iron transporting scavenger protein SCARA5.

Most investigations of intrathecally produced antibodies in MS have focussed on IgG, however, intrathecal IgM synthesis is associated with a more active inflammatory disease phenotype,^{6,15} a higher likelihood of conversion from CIS to clinically definite MS,^{7,16–18} and spinal manifestation, suggesting a distinct clinical phenotype and pathophysiology.^{8,19} Intrathecal IgM is also associated with increased complement activation in the CSF, especially of the early classical and alternative pathways (Oechtering et al., under revision). This observation implies that the IgM must find antigen in the CNS because complement activation by IgM in the classical pathway requires a multimeric cognate interaction between multiple Fab domains and their targets.²⁰

Additional evidence for an antigen-driven intrathecal origin of the anti-PNET IgM includes the fact that B3, like the IgM antibodies described by Beltrán et al.,⁹ shows CDR-enriched somatic hypermutation, and that antigen-binding is dependent on this mutation.

The transcriptional profile of the B cell giving rise to B3 was partially typical of a plasma cell. The high expression of HLA genes seen in this B cell is also consistent with a plasma cell phenotype and has been associated with freshly generated, antigen-specific plasma cells thought to be pathogenic in systemic lupus erythematoses.²¹ High expression of GPR183 by B3 was unexpected. GPR183 is thought to be involved in directing B cell migration within lymph nodes²² and has more recently been shown to contribute to tissue homing and antibody secretion by plasma cells in the gut.²³

SCARA5 functions as a transferrin-independent ferritin receptor for both iron delivery and ferritin removal.^{24,25} Dysregulation of iron metabolism and the resultant cytotoxicity is increasingly implicated in MS.²⁶ Elevated transcripts of SCARA5, as well as of other iron import-related molecules, were described in MS lesions, especially in the peri-plaque white matter, suggesting a cellular defence

Figure 3 Continued

the log₁₀ maximum number of reads found in the other B cell lines (light blue dots). Genes whose expression is significantly higher in PNET (two-tailed, unpaired *t*-test, $P < 1 \times 10^{-8}$), and whose GO terms include 'plasma membrane' are marked with red circles and their gene symbols printed adjacent to the plotted. (D) Binding of B3 to cells transfected with either PCDH18 or SCARA5 measured by flow cytometry. B3 non-binding HEK cells were transfected with plasmids mediating expression of either PCDH18 (left) or SCARA5 (right) and co-transfected with fluorescent protein transfection markers (mCherry for PCDH18 and GFP for SCARA5). Vertical axis of each contour plot shows B3 binding and horizontal axis shows transfection marker. (E) Impact of isoform. Analogous experiments to D were conducted using HEK cells transfected with each of the 176-, 400- and 495 amino acid isoforms of SCARA5. Vertical axis shows binding of a commercial mouse anti-human SCARA5 antibody (left plots) or B3 (right plots). Horizontal axis shows forward scatter (no transfection marker used in this experiment). Blue contours are results with the commercial or B3 antibody, red contours are results from cells incubated with the appropriate secondary antibody only. (F) Prevalence of IgM antibodies against PNET cells and against SCARA5 in a cohort of donors with various diagnoses. Vertical axis shows IgM binding. Six sections left to right show results from donors with different diagnoses (left to right: CIS, PPMS, RRMS, SPMS, healthy controls, inflammatory non-MS, as specified within each plot). Within each of the six plots, the left-most column shows binding to HEK cells transfected with the 495-amino acid isoform, the middle column binding to the 176-amino acid isoform, and the right column binding to PNET cells. (G) Binding of antibodies from serum to SCARA5-expressing cells. Vertical axis shows GMFI ratio (antibody + secondary-labelled cells divided by cells labelled with secondary antibody only obtained from SCARA5-HEK cells, again divided by the same value obtained from untransfected HEK cells). Each separate plot represents binding IgG (on the left), IgA (in the middle) or IgM (on the right) from serum samples from donors with CIS (black), MS (red) and controls (blue). Comparison of antibody binding between different diagnosis was performed by one-way ANOVA. CIS = clinically isolated syndrome; infl. CTRL = inflammatory control; ns = not significant; PPMS = primary progressive multiple sclerosis; RRMS = relapsing remitting multiple sclerosis; SPMS = secondary progressive multiple sclerosis.

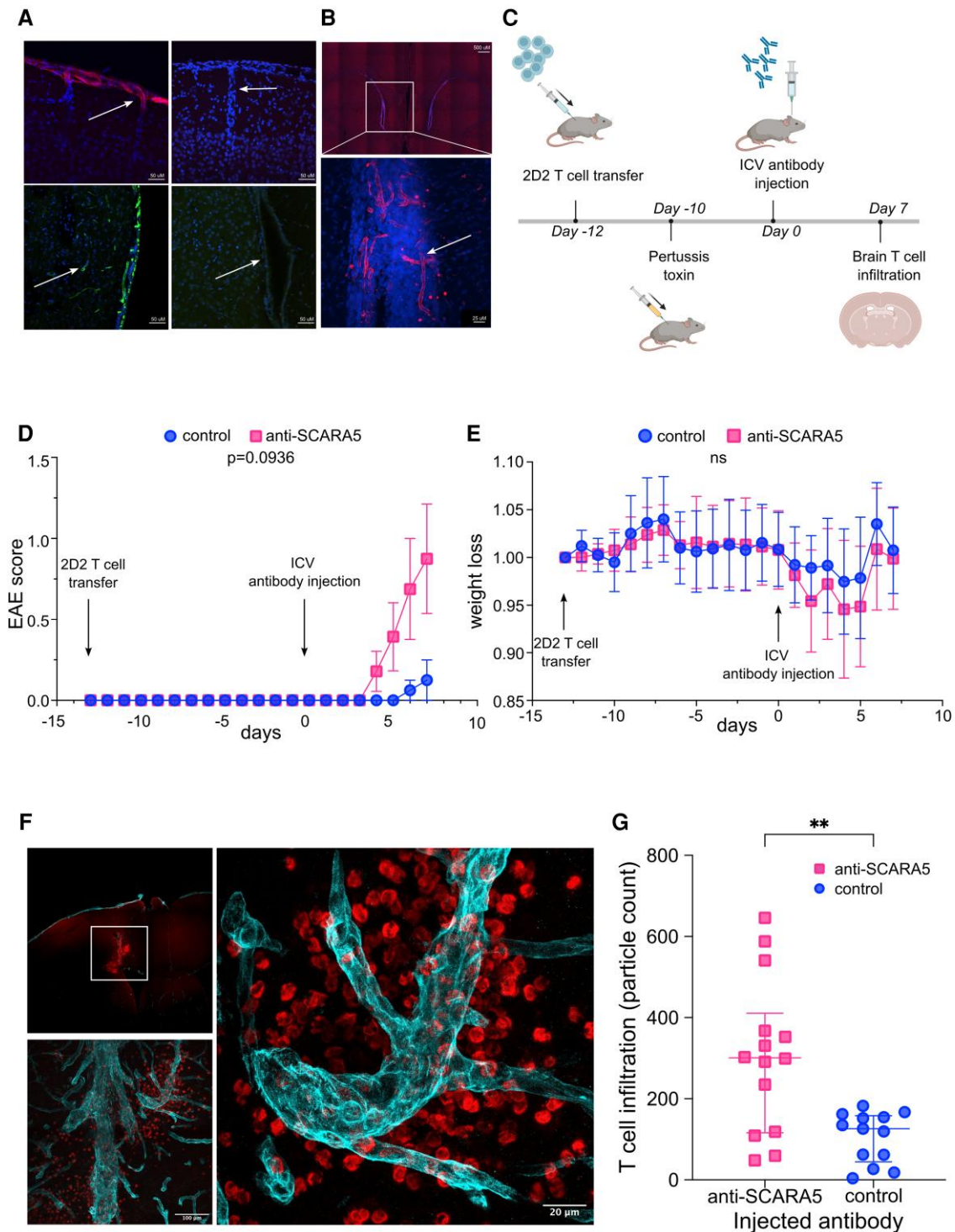


Figure 4 Impact of anti-SCARA5 antibodies on immune cell trafficking into brain. (A) Immunofluorescent labelling of SCARA5 expression in mouse brain. Vibratome sections from perfusion-fixed brains of unmanipulated mice were immunolabelled with sheep anti-SCARA5 antibodies and visualized by confocal microscopy. Two upper images show surface (subdural) and penetrating blood vessels of the superficial cortex. The upper left image shows nuclei labelled with DAPI in blue and immunolabelling for SCARA5 in red. The upper right image shows a similar location from a control section, from which the primary antibody was omitted, imaged with the same parameters. In the lower two images, labelling of periventricular blood vessels is shown. The left image is labelled with sheep anti-SCARA5 (green) and the right is a no-primary control. (B) Anti-SCARA5 binding to live blood vessels. A polyclonal sheep anti-SCARA antibody was injected into the lateral ventricle of a mouse and the next day the mouse was sacrificed by perfusion fixation, and the brain labelled with DAPI (blue) and anti-sheep secondary antibody (red). The upper panel is a composite image made by stitching together images captured with a 10× objective, to show both the ventricles—the ventricle highlighted with a box on the left received the injection. The panel below is a maximum intensity projection of a confocal stack of the area shown in the box, captured with the 40× objective showing the blood vessels in the wall of the ventricle labelled by the *in vivo* antibody injection. (C–G) Impact of intraventricular anti-SCARA5 antibodies on encephalitic T cell infiltration. All figures show results pooled from three experiments, each with 3–6 animals per group. (C) Schematic diagram of experimental design

(Continued)

Figure 4 Continued

(created with BioRender.com). *In vitro* activated, MOG-specific 2D2 T cells were transferred to recipient animals by intraperitoneal injection, followed by pertussis toxin, and animals were tracked until the first animals showed motor signs, at which point, the remaining asymptomatic animals were randomized into two groups to receive anti-SCARA5 antibody or control. (D) Motor impairment of animals over time. Motor function was subjectively assessed according to a system used for scoring experimental autoimmune encephalomyelitis (EAE), in which 0 is unimpaired, and 4 is severe impairment. Points show the means within the conditions and the bars the standard error of the mean (SEM). Red squares indicate the animals injected with anti-SCARA5 antibody and blue circles control animals injected with PBS or control antibody. $P = 0.0936$ calculated by two-tailed unpaired t-test between the areas under the curves for each condition. (E) Weights of animals over time of experiment. Weights are expressed as the weight at each time point divided by the weight at the start of the experiment for each animal. Points show the means within the conditions and the bars the SEM. Purple circles represent control animals and blue squares the animals injected with anti-SCARA5. (F) T cell infiltration. Vibratome section of brain from animals sacrificed at 1 week after intraventricular antibody injection in the experiment described above were immunolabelled for laminin (blood vessel walls, red) and CD3-epsilon (T cells, green). (G) Quantification of infiltrating T cells. Images like the ones shown in F were captured for 5–6 sections per mouse by an automated fluorescent microscope and the numbers of T cells per section extracted by an automated script in ImageJ. Points show the median number of T cells per section for each mouse and the whiskers show the interquartile range. $**P = 0.0012$, two-tailed unpaired t-test. ns = not significant.

response against iron toxicity.²⁷ Soluble SCARA5 was also significantly reduced in the CSF of patients with MS compared to controls.²⁸ Considering the expression of SCARA5 in brain endothelial cells and choroid plexus, we hypothesized that anti-SCARA5 antibodies could exert their pathogenic effect by influencing immune cell trafficking into the brain. Intrathecal application of a SCARA5 antibody indeed had an influence on T cell infiltration in an experimental autoimmune encephalomyelitis (EAE) model using MOG-specific T cells. The identified target SCARA5 suggests that the pathogenetic role of these antibodies could rely on the initiation of blood–brain barrier breakdown and in the facilitation of CNS immune cell infiltration, pointing to a direct involvement in causing the disease, rather than to an epiphenomenon associated with cell death.

PNET IgM is more frequently seen in younger patients. This suggests an association with the inflammatory phase of MS and might represent the signature of an antibody response happening early in the disease course, potentially present even before clinical onset of the disease, as has been reported for other autoantibodies such as AQP4 and GAD in neuromyelitis optica (NMO) and type 1 diabetes, respectively.^{29,30}

As the proportion of patients with anti-PNET IgM in CSF is much larger than the population with anti-SCARA5 reactivity, there must be a large population of patients with antibodies binding some other epitope on the PNET cells. One possibility is that SCARA5 is one protein in a complex that is the target of the MS-specific antibody response. However, SCARA5 is not an intensely studied protein and its binding partners have yet to be characterized, so additional studies will be required to investigate this possibility.

Data availability

All data produced in this study will be made publicly available by the time of publication, with the exception of human sequence data with the potential to infringe donors' rights to withdraw consent for their data to be made public. In particular, the complete coding sequences of heavy and light chains of the antibodies described can be found at ncbi (accession number OQ744174.1 to OQ744183.1).

Acknowledgements

We thank the patients and staff of the University Hospital Basel and the University Hospital of Graz for their participation in the study. We thank Barbara Treutlein and Ryoko Okamoto for the provision of cells for testing antibodies. We thank Rachel Lindemann for the support in conducting some of the animal experiments.

Sample collection was made possible by the Swiss Multiple Sclerosis Cohort organisation, supported in part by the Swiss Multiple Sclerosis Society. We are also grateful for technical support from the flow cytometry, microscopy, and bioinformatics core facilities of the Department of Biomedicine, and computational resources provided by the scientific computing center of the University of Basel (<http://scicore.unibas.ch/>).

Funding

Funding was provided by the Swiss Multiple Sclerosis Society (N.S.R.S.) and by the Swiss National Science Foundation grant number 189043 (T.D.). I.C. received funding from the European Academy of Neurology. M.D. received funding from the Swiss National Science Foundation [project-number 199310] and the German Research Foundation [IMM-PACT-programme, 413517907].

Competing interests

M.K. has received funding for attending meetings or travel from Merck and Biogen, honoraria for lectures or presentations from Novartis and Biogen and speaker serves on scientific advisory boards for Biogen, Merck, Roche, Novartis, Bristol-Myers Squibb, and Gilead. He received research grants from Biogen and Novartis. L.K. discloses research support to his institution (University Hospital Basel): steering committee, advisory board, and consultancy fees (Actelion, Bayer HealthCare, Biogen, BMS, Genzyme, Janssen, Merck, Novartis, Roche, Sanofi, Santhera, and TG Therapeutics); speaker fees (Bayer HealthCare, Biogen, Merck, Novartis, Roche, and Sanofi); support of educational activities (Allergan, Bayer HealthCare, Biogen, CSL Behring, Desitin, Genzyme, Merck, Novartis, Pfizer, Roche, Sanofi, Shire, and Teva); license fees for Neurostatus products; and grants (Bayer HealthCare, Biogen, European Union, InnoSwiss, Merck, Novartis, Roche, Swiss MS Society, and Swiss National Research Foundation). J.K. received speaker fees, research support, travel support, and/or served on advisory boards by Swiss MS Society, Swiss National Research Foundation (320030_189140/1), University of Basel, Progressive MS Alliance, Bayer, Biogen, Bristol Myers Squibb, Celgene, Merck, Novartis, Octave Bioscience, Roche, Sanofi. T.D. received financial compensation for participation in advisory boards, steering committees and data safety monitoring boards, and for consultation for Alexion, Novartis Pharmaceuticals, Merck, Biogen, Celgene, GeNeuro, MedDay, Mitsubishi Tanabe Pharma, Roche, and Sanofi Genzyme. T.D. also received research support from Alexion, Roche, Biogen, National Swiss Science Foundation, European Union, and Swiss MS Society.

Supplementary material

Supplementary material is available at *Brain* online.

References

- Berek K, Hegen H, Auer M, Zinganell A, Di Pauli F, Deisenhammer F. Cerebrospinal fluid oligoclonal bands in neuroborreliosis are specific for *Borrelia burgdorferi*. *PLoS One*. 2020; 15(9):e0239453.
- Meinl E, Krumbholz M, Hohlfeld R. B lineage cells in the inflammatory central nervous system environment: Migration, maintenance, local antibody production, and therapeutic modulation. *Ann Neurol*. 2006;59:880-892.
- Reiber H, Ungefehr S, Jacobi C. The intrathecal, polyspecific and oligoclonal immune response in multiple sclerosis. *Mult Scler*. 1998;4:111-117.
- Villar LM, Masjuan J, Sádaba MC, et al. Early differential diagnosis of multiple sclerosis using a new oligoclonal band test. *Arch Neurol*. 2005;62:574-577.
- Capuano R, Zubizarreta I, Alba-Arbalat S, et al. Oligoclonal IgM bands in the cerebrospinal fluid of patients with relapsing MS to inform long-term MS disability. *Mult Scler*. 2021;27:1706-1716.
- Villar LM, Masjuan J, González-Porqué P, et al. Intrathecal IgM synthesis predicts the onset of new relapses and a worse disease course in MS. *Neurology*. 2002;59:555-559.
- Huss A, Abdelhak A, Halbgebauer S, et al. Intrathecal immunoglobulin M production: A promising high-risk marker in clinically isolated syndrome patients. *Ann Neurol*. 2018;83:1032-1036.
- Oechtering J, Schaedelin S, Benkert P, et al. Intrathecal immunoglobulin M synthesis is an independent biomarker for higher disease activity and severity in multiple sclerosis. *Ann Neurol*. 2021;90:477-489.
- Beltrán E, Obermeier B, Moser M, et al. Intrathecal somatic hypermutation of IgM in multiple sclerosis and neuroinflammation. *Brain*. 2014;137:2703-2714.
- Obermeier B, Mentele R, Malotka J, et al. Matching of oligoclonal immunoglobulin transcriptomes and proteomes of cerebrospinal fluid in multiple sclerosis. *Nat Med*. 2008;14:688-693.
- Obermeier B, Lovato L, Mentele R, et al. Related B cell clones that populate the CSF and CNS of patients with multiple sclerosis produce CSF immunoglobulin. *J Neuroimmunol*. 2011;233(1-2): 245-248.
- Uy CE, Binks S, Irani SR. Autoimmune encephalitis: Clinical spectrum and management. *Pract Neurol*. 2021;21:412-423.
- Lily O, Palace J, Vincent A. Serum autoantibodies to cell surface determinants in multiple sclerosis: A flow cytometric study. *Brain*. 2004;127:269-279.
- Mapunda JA, Tibar H, Regragui W, Engelhardt B. How does the immune system enter the brain? *Front Immunol*. 2022;13:805657.
- Villar LM, Masjuan J, González-Porqué P, et al. Intrathecal IgM synthesis is a prognostic factor in multiple sclerosis. *Ann Neurol*. 2003;53:222-226.
- Pfuhl C, Grittner U, Gieß RM, et al. Intrathecal IgM production is a strong risk factor for early conversion to multiple sclerosis. *Neurology*. 2019;93:e1439-e1451.
- Ozakbas S, Cinar BP, Özcelik P, Baser H, Kosehasanoğullari G. Intrathecal IgM index correlates with a severe disease course in multiple sclerosis: Clinical and MRI results. *Clin Neurol Neurosurg*. 2017;160:27-29.
- Perini P, Ranzato F, Calabrese M, Battistin L, Gallo P. Intrathecal IgM production at clinical onset correlates with a more severe disease course in multiple sclerosis. *J Neurol Neurosurg Psychiatry*. 2006;77:953-955.
- Oechtering J, Lincke T, Schaedelin S, et al. Intrathecal IgM synthesis is associated with spinal cord manifestation and neuronal injury in early MS. *Ann Neurol*. 2022;91:814-820.
- Sharp TH, Boyle AL, Diebold CA, Kros A, Koster AJ, Gros P. Insights into IgM-mediated complement activation based on in situ structures of IgM-C1-C4b. *Proc Natl Acad Sci U S A*. 2019; 116:11900-11905.
- Jacobi AM, Mei H, Hoyer BF, et al. HLA-DRhigh/CD27high plasmablasts indicate active disease in patients with systemic lupus erythematosus. *Ann Rheum Dis*. 2010;69:305-308.
- Pereira JP, Kelly LM, Xu Y, Cyster JG. EB12 mediates B cell segregation between the outer and centre follicle. *Nature*. 2009;460: 1122-1126.
- Ceglia S, Berthelette A, Howley K, et al. An epithelial cell-derived metabolite tunes immunoglobulin A secretion by gut-resident plasma cells. *Nat Immunol*. 2023;24:531-544.
- Li JY, Paragas N, Ned RM, et al. Scara5 is a ferritin receptor mediating non-transferrin iron delivery. *Dev Cell*. 2009;16:35-46.
- Yu B, Cheng C, Wu Y, et al. Interactions of ferritin with scavenger receptor class A members. *J Biol Chem*. 2020;295: 15727-15741.
- Tham M, Frischer JM, Weigand SD, et al. Iron heterogeneity in early active multiple sclerosis lesions. *Ann Neurol*. 2021;89:498-510.
- Hametner S, Wimmer I, Haider L, Pfeifenbring S, Brück W, Lassmann H. Iron and neurodegeneration in the multiple sclerosis brain. *Ann Neurol*. 2013;74:848-861.
- Johansson D, Rauld C, Roux J, et al. Mass cytometry of CSF identifies an MS-associated B-cell population. *Neurol Neuroimmunol Neuroinflamm*. 2021;8:e943.
- Nishiyama S, Ito T, Misu T, et al. A case of NMO seropositive for aquaporin-4 antibody more than 10 years before onset. *Neurology*. 2009;72:1960-1961.
- Tuomilehto J, Vidgren G, Toivanen L, et al. Antibodies to glutamic acid decarboxylase as predictors of insulin-dependent diabetes mellitus before clinical onset of disease. *Lancet*. 1994; 343:1383-1385.